IJST, Transactions of Civil Engineering, Vol. 37, No. C2, pp 243-256
Printed in The Islamic Republic of Iran, 2013

EFFECTS OF DIFFERENT FREQUENCY CONTENT OF MULTI-SUPPORT EXCITATIONS ON SEISMIC RESPONSE OF A LARGE EMBANKMENT DAM*

S. M. A. SADROLDDINI[1**], M. DAVOODI[2] AND M. K. JAFARI[3]

[1]Dept. of Civil Engineering, Science and Research Branch, Islamic Azad University, Tehran, I. R. Iran
Email: Ali_civil75@yahoo.com
[2, 3]International Institute of Earthquake Engineering and Seismology, 26 Arghavan St., N. Dibajie, Farmanieh
Tehran, I. R. Iran

Abstract– This paper focuses on examining the combined effects of frequency content and spatial variability of the ground motion on the response of a large embankment dam. A series of non-uniform ground motion time histories are generated using spectral representation method. The influence of frequency content of seismic excitation is taken into account by using three different types of target response spectra selected from Uniform Building Code (UBC 1994). It is found that the use of identical ground motions compatible with the Types 1 and 2 response spectra overestimates the acceleration responses by up to 15% and 30% higher than those of multi-support excitations, respectively. The above trend is qualitatively valid for Type 3 input motions at lower elevations of the dam, but not at the crest of the dam where the uniform excitation yields slightly lower acceleration response. By comparing the displacement responses, it is demonstrated that the uniform input motions compatible with Types 1, 2 and 3 response spectra result in 10%, 35% and 40% larger crest settlements, respectively, than those predicted under multi-support excitations.

Keywords– Embankment dam, multi-support excitation, frequency content, response spectra

1. INTRODUCTION

Analysis of recorded data at dense instrument arrays indicates that the ground motion spatial variations are significant for distances comparable to the length of the majority of large structures [1]. Newmark and Rosenblueth [2] stated that even for short span structures there is a tendency for their supports to move differentially. Therefore, for relatively long structures such as embankment dams the effects of earthquake-induced differential motions at foundation level become a problem of interest. To consider this effect, spatially variable seismic ground motions at the different points along the base of the dam should be estimated.

The Spatial Variation of Earthquake Ground Motion (SVEGM) is commonly attributed to the combination of three different phenomena: a) incoherence effects due to wave scattering or extended source effects; b) wave passage effects, which is the difference in arrival times of the seismic waves at different stations; c) Local site effects which arise from the differences in local soil conditions [3].

Seismic response analysis of long-span structures under multi-support excitations has been the subject of extensive investigations during the past decades. A comprehensive literature review of the effects of SVEGM on the seismic response of concrete and embankment dams was conducted by Davoodi et al. [4]. Results of past studies indicated that the stress responses of concrete gravity dams calculated

*Received by the editors July 3, 2011; Accepted October 7, 2012.
**Corresponding author

from the spatially varying earthquake ground motions are larger than those at the uniform ground motion [4].

Maheri and Ghaffarzadeh [5] studied the effects of asynchrony and non-uniformity of support's motion on the response of a concrete gravity dam and other structures. They concluded that the non-uniformity may, in some cases, amplify the effects of asynchrony and therefore should be considered in the analysis.

Haroun and Abdel Hafiz [6] investigated the effects of amplitude and phase difference of an earthquake motion on the seismic response of long earth dams. They found that the uniform excitation produces the maximum response for dams with small length-to-height ratios, whereas the variable amplitude excitation yields the maximum response at the mid-point of the dam for relatively large length-to-height ratios.

Chen and Harichandran [7] studied the effect of SVEGM on the response of Santa Felicia earth dam using a linear random vibration method. Their results indicated that the stress response of stiff material near the base of the dam can be significantly increased due to SVEGM. They also found that SVEGM slightly decreases the displacement and strain response of the dam. They expressed that the use of identical excitations is adequate and conservative as far as predicting the displacement and strain response of the dam. The beneficial effect of ground motion incoherence on the response of rockfill dams in rigid-oscillating narrow canyons was also expressed by Gazetas and Dakoulas [8].

Davoodi and Javaheri [9] studied the effect of SVEGM on the stochastic response of Masjed Soleyman embankment dam. They concluded that SVEGM can have a significant effect on the stability of embankment dams. Davoodi et al. [4] investigated the sensitivity of the Masjed Soleyman dam responses to the ground motion incoherence by using three different coherency models. They concluded that higher coherency decay yields lower acceleration and displacement responses of the dam.

Many authors have explained that the differences in the dam responses to uniform and SVEGM excitations are mainly due to the so-called pseudo-static response of the dam [7, 10]. The pseudo-static response is that which would occur if ground motions were applied very slowly to make inertia and damping effects negligible [10]. It should be mentioned that the separation of pseudo-static and relative responses is possible by using the finite element formulation. In this method, the dynamic equations of motion of a structure are discretized such that the pseudo-static displacements are obtained by neglecting the inertia and damping forces. Detailed description of this method can be found in [5]. In the present study, the dynamic response of the dam is calculated using finite difference method in which the pseudo–static responses cannot be obtained by the above mentioned method.

The influence of the frequency characteristics of the excitation on the nonlinear response of a broad range of earth dams was studied by Gazetas et al. [11]. They concluded that the distribution of response quantities within the dam was quite sensitive to predominant ground frequency. Popsecu [12] found that the interplay between the frequency content of seismic excitation and the dynamic characteristics of the soil system and their evolution during and after the earthquake have important implications on the dynamic response.

Most previous studies on determining the ground motion spatial variation effects on structural responses concerned only specific frequency content of seismic excitations. In other words, the possible effect of frequency content of input motion on the response of structures to multi-support excitation has not been considered properly. The purpose of this study is to gain insight into the effects of the spatial variability of ground motion on the response of large embankment dams. To consider the influence of frequency content of seismic excitations, the non-uniform acceleration time histories were generated compatible with different spectral properties. The Masjed-Soleyman embankment dam, constructed in Iran was selected as a numerical example. The spatially varying earthquake ground motion model includes both incoherence and wave-passage effects. Numerical analyses were conducted using the finite difference program FLAC 5.0 code (Itasca, 2005) based on a continuum finite difference discretization using the Langrangian approach.

2. DESCRIPTION OF THE SIMULATION TECHNIQUE FOR GENERATING SVEGM

Interestingly, various international seismic codes allow the use of simulated ground motion time histories for the seismic design of structures. For this purpose, the simulated time-histories have to be spectrum-compatible, i.e. the average response spectrum computed using simulated time histories has to match the target response spectrum provided by the code over a fixed frequency range and with a code-specified tolerance [13].

In this study, the spectral representation technique [14] is used to generate spatially varying ground motion time histories that are compatible with a prescribed response spectrum. In this method, the stationary stochastic vector process *fj(t)* at each station *j* can be simulated by the following series:

$$f_j\ (t) = 2\sum_{m=1}^{j}\ \sum_{l=1}^{N} \left| H_{jm}(\omega_l,t) \right| \sqrt{\Delta\omega}\cos\left[\omega_l t - \theta_{jm}(\omega_l,t) + \phi_{ml}\ \right] \quad j = 1,2,3,4,...,M \tag{1}$$

Where:

$$\omega_l = l\,\Delta\omega \qquad l = 1,2,...,N\ ,\quad \Delta\omega = \frac{\omega_u}{N} \tag{2}$$

$$\theta_{jk}(\omega) = \tan^{-1}\left[\frac{\mathrm{Im}\left[H_{jk}(\omega)\right]}{\mathrm{Re}\left[H_{jk}(\omega)\right]}\right] \tag{3}$$

In Eq. (1) to (3), *M* is the total number of spatial stations, *H(ω,t)* is a lower triangular matrix obtained by cholesky decomposition of cross spectral density matrix at every time instant t, φ_{ml} are sequences of random phase angles uniformly distributed over the range [0,2π], ω_u represents an upper cut-off frequency, Δω is the resolution in the frequency domain, *N* is the total number of frequency samples, and *Im[Hjk(ω,t)]* and *Re[Hjk(ω,t)]* are the imaginary and real parts of the *H(ω,t)*, respectively. The elements of the cross spectral density matrix are defined as:

$$S_{jk}{}^{0}(\omega,t) = A_j(t)A_k(t)\sqrt{S_j(\omega)\ S_k(\omega)}\ \gamma_{jk}(\omega)\exp[-\frac{i\omega v}{V_s}] \quad j,k = 1,2,3,4,...,M \tag{4}$$

where $S_{jk}(\omega)$ are cross spectrum of the motions between the two stations *j* and *k*, $A_j\ (t)$ are uniform modulating functions, $\gamma_{jk}(\omega)$ are the coherence functions between the ground motions generated at stations *j* and *k, v* is separation distance and V_s is velocity of shear wave propagation. After multiplying the generated stationary time histories by appropriate envelope functions to introduce non-stationarity, an iterative scheme is used to match generated time histories to target response spectrum [3]. It is important to emphasize that the non-uniform acceleration time histories at ground surface are generated compatible with the three prescribed target quantities: (1) target response spectra, (2) complex coherence function, and (3) modulating functions.

To include different characteristics of input motions, three types of response spectra defined by Uniform Building Code (UBC 1994) are used as target spectra for ground motion generation. Three different types of the UBC response spectra including Type 1 (S1) for rock and stiff soils, Type 2 (S2) for deep cohesionless or stiff clay soils, and Type 3 (S3) for soft to medium clays and sands are shown in Fig.

1. It must be noted that the peak ground acceleration for Maximum Credible Level (MCL) is set equal to 0.45g. The selected value of a_{max}=0.45g is consistent with the results of a seismic hazard study and is predicted for a return period of 2000 years [15].

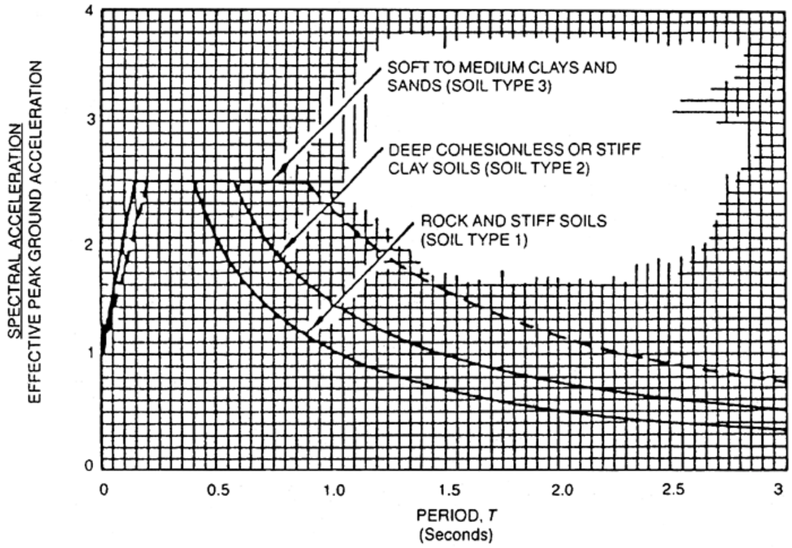

Fig. 1. Three types of UBC (1994) response spectra selected for ground motion generation

Spatially incoherent seismic ground motions are generated based on the widely used coherency model proposed by Harichandran-Vanmarcke [16]. This model is based on the study of four events recorded by the SMART-1 array in Taiwan:

$$|\gamma(\upsilon,\omega)| = A\exp\left[-\frac{2\upsilon}{\alpha\theta(\omega)}(1-A+\alpha A)\right]+(1-A)\exp\left[-\frac{2\upsilon}{\theta(\omega)}(1-A+\alpha A)\right] \tag{5.1}$$

Where

$$\theta(\omega) = k\left[1+(\omega/\omega_0)^b\right]^{-1/2} \tag{5.2}$$

In which A, α, κ, ω_o and b are the model parameters. These parameters were estimated by Harichandran and Wang [17] as A=0.626; α = 0.022; k = 19700; ω_0 = 12.692 and b=3.47. As for other multiple-parameters models, this model can be made to match a broad range of coherency applications. It is assumed that the horizontal seismic waves propagate across the dam foundation with the wave velocity of 1200 m/s. As a third target quantity, the Jennings et al. [18] envelope function is used for the modulation purpose.

3. NUMERICAL MODEL

The Masjed Soleyman embankment dam is located in the Zagros Mountains in Khuzestan, southwest of Iran. The dam has a maximum height of 177m, width of 700m at the foundation level and crest length of 492m. It is made of a central impervious core and pervious shell upstream and downstream. The maximum cross-section of the dam and its material zones are shown in Fig. 2. Extensive laboratory and field tests were carried out prior and after construction of the dam to characterize the embankment and foundation materials. Table 1 summarizes the material properties selected for dynamic analysis of the dam.

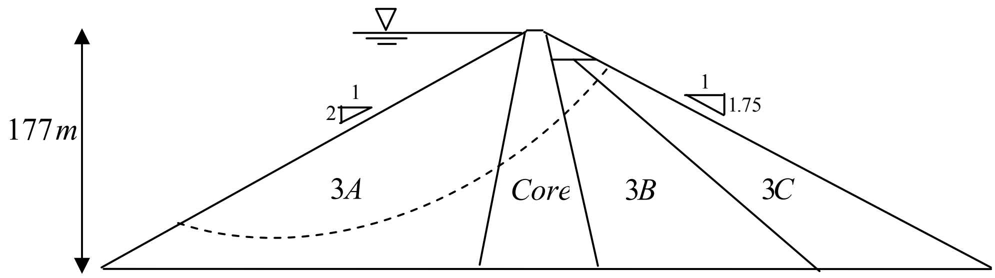

Core: Impervious clayeysoils
3A: Shell (Rockfill)- Predominately conglomerate, max particlesize 1000 mm.
3B: Shell (Rockfill)- Conglomerate with sandstone and clayey siltstone, max particlesize 1000 mm.
3C: Shell (Rockfill)- Conglomerate with sandstone, max particlesize 1000 mm.
Foundation: conglomerate, claystone, sandstone and siltstone.

Fig. 2. Maximum cross section, material zones and slip surface of the upstream slope of the Masjed Soleyman embankment dam

Table 1. Material properties of the earth dam used in numerical analysis [19]

Material		Density (ton/m^3)	Poisson ratio υ	φ' (deg)	C' (kPa)
Core		2.20	0.45	30.0	0.0
3A	Saturated	2.35	0.40	45.0	0.0
	Unsaturated	2.20	0.40		
3C	Saturated	2.35	0.40	45.0	0.0
	Unsaturated	2.20	0.40		
3B	Unsaturated	2.2	0.40	37.0	0.0
Foundation		2.5	0.30	40.0	0.0

Figure 3 compares the dependency of soil stiffness on strain level for core and shell materials as observed in dynamic laboratory tests [19] and obtained by the Flac default hysteretic function. As can be seen in Fig. 3, the program default hysteretic model provides a reasonable fit to both core and shell modulus-reduction curves over the whole range of strains. Jafari and Davoodi [20] have evaluated the modified profile of small strain shear modulus in the dam body using a seismic refraction survey on the dam body, the right and the left abutments. Applying the results of this study, the profile of the shear wave velocity used in the present study is shown in Fig. 4.

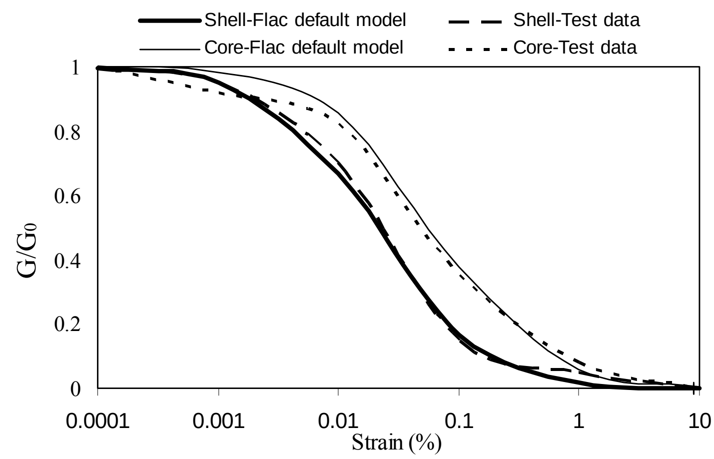

Fig. 3. Variation of shear modulus with strain for core and shell materials [19]

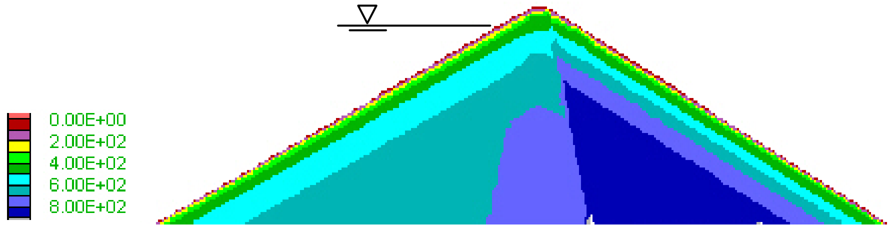

Fig. 4. Variation of the shear wave velocity at various depths in the dam (m/s) [20]

The finite difference analyses were carried out adopting hysteretic damping and elastic-perfectly plastic Mohr-Coulomb material behaviour. To avoid numerical distortion of the propagating wave during the dynamic analysis, the maximum height of elements of the dam (Δl_{max}=7.5m) is smaller than 1/5 of the wavelength λ_{min} associated with the highest frequency component of the input wave fmax [21]. The depth and lateral extent of the foundation and the boundary conditions along the vertical and horizontal edges of the finite difference model are illustrated in Fig. 5. The sequences of steps involved in construction of the embankment and development of seepage through it have little or no effect on the long term static stresses in the embankment [22]. As a result, the analysis procedure can be simplified. In this study, the initial stress distribution in the dam body is calculated by full embankment method. In this method the dam is not divided into horizontal slices but the stresses are calculated by one time procedure. Seepage analysis was performed to achieve steady state conditions within the embankment and the foundation. Fundamental equations of seepage analysis can be found in [23].

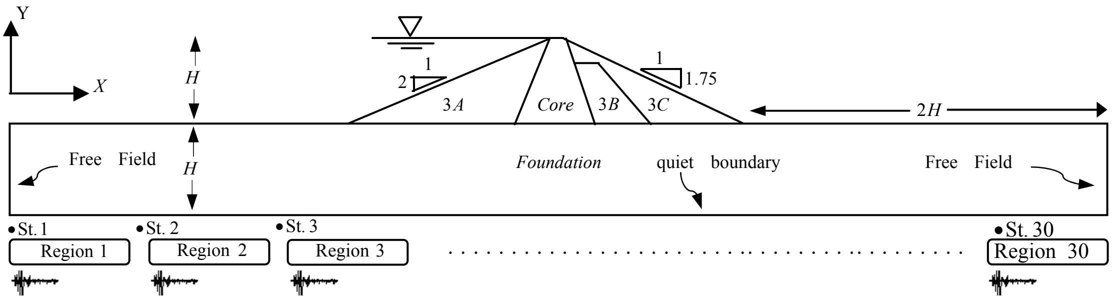

Fig. 5. Geometry, boundary conditions of numerical model and configuration of base divisions for multi-support excitation

4. MULTI-SUPPORT EXCITATION AND DYNAMIC LOADING CASES

For multi-support excitation, the base of the dam is divided into a number of regions. The generated spatially variable seismic ground motions were then applied at each region at the base of the dam. It is assumed that all support points located within a region have identical excitation. To determine the appropriate number of base divisions, the sensitivity of the dam response to the number of loading regions at the base is evaluated by considering 5, 10, 15, 20, 30 and 40-region cases.

Figure 6 compares the variation of acceleration responses of the dam with the number of loading regions at different elevations along the centre line of the dam. Comparisons are in terms of the Root Mean Squares (RMS) of the computed acceleration time histories. It is apparent from this figure that as the number of base subdivisions exceeds 30 regions, the variation in the acceleration responses becomes negligible at all elevations. Therefore, in this study, the base of the dam is divided into 30 loading regions for multi-support excitation. The configuration of the stations and the base regions is presented in Fig. 5 for 30-region case. The generated motions at each station have then been applied at each loading region presented in Fig. 5.

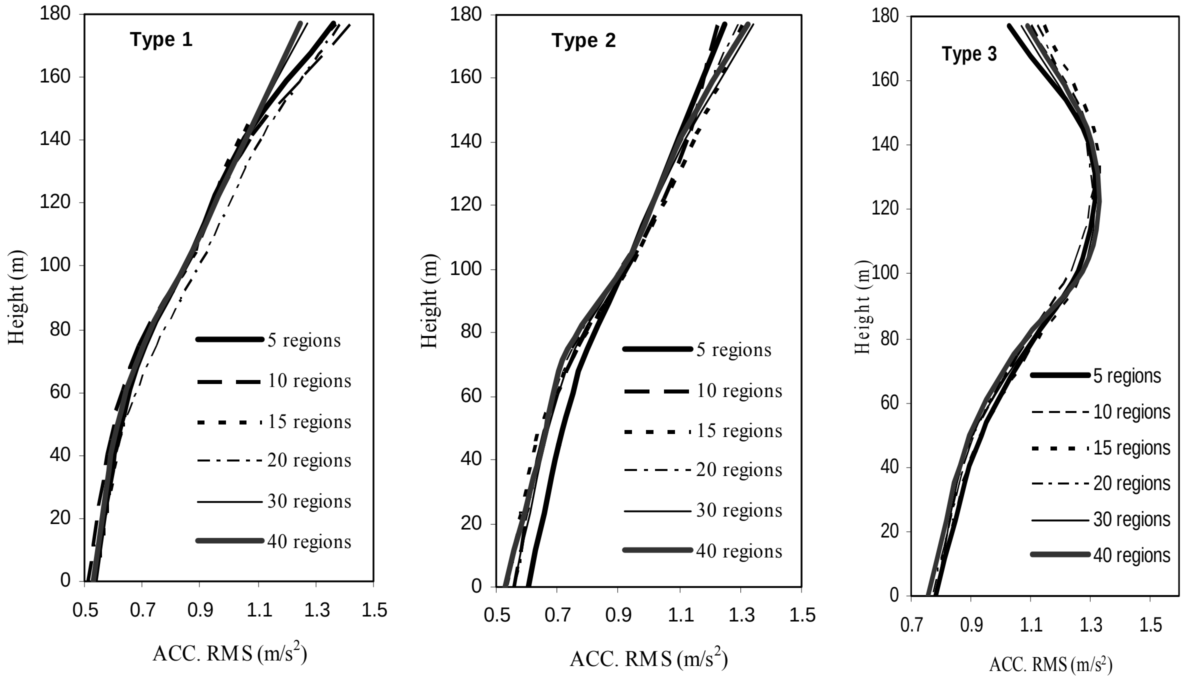

Fig. 6. The variation of the dam acceleration response with the number of loading regions at different elevations along the centre line of the dam

According to the three different types of target response spectra introduced in section 2, three types of input motions, each including both uniform and SVEGM motions were generated and used as input motions. Table 2 describes in more detail the loading cases considered in this study, regarding the different characteristics of generated excitations. To demonstration, the generated ground motion time histories at the station No. 3 are shown in Fig. 7. Space limitations preclude the presentation of all the generated motions at all stations. In Fig. 8 the response spectra of the generated records are compared with the target one. It can be inferred that the generated time histories are in a good agreement with the target response spectra. It is to be noted that, due to the same frequency contents and intensities of uniform and SVEGM motions, the only difference between the motions of different stations can be attributed to the incoherence and wave passage effect.

Table 2. Detailed description of different types of input motions

Types of input motions	Target response spectrum	Description of input motions
Type1	UBC-Type 1	Uniform- Type1
		SVEGM - Type1
Type2	UBC-Type 2	Uniform- Type2
		SVEGM - Type2
Type3	UBC-Type 3	Uniform- Type3
		SVEGM - Type3

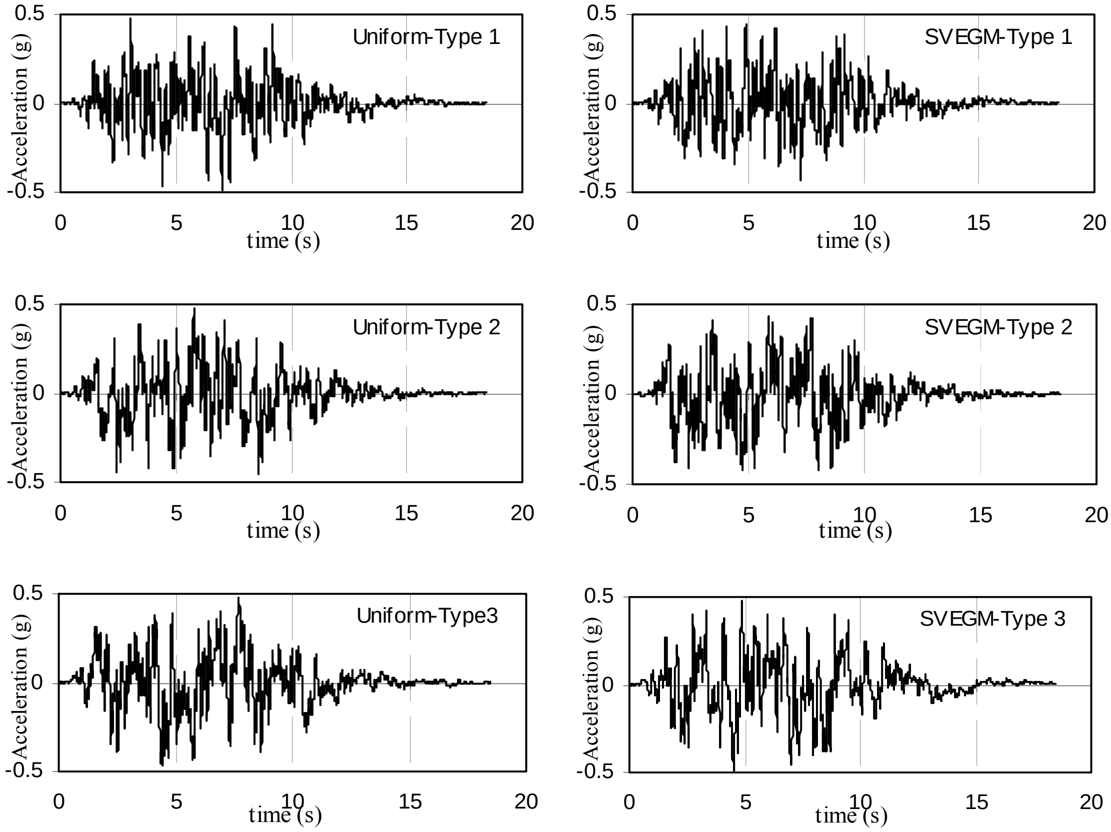

Fig. 7. Generated acceleration time histories at station No.3 compatible to prescribed target response spectra introduced in Table (2)

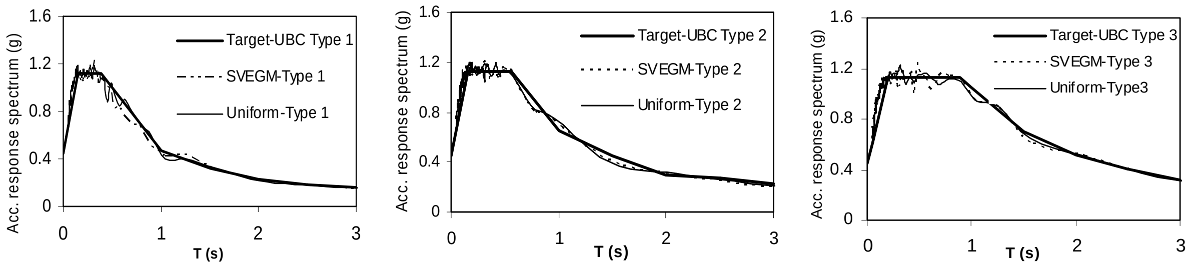

Fig. 8. Response spectrum comparison of generated records with the target one at station No.3 for three types of uniform and SVEGM excitations

5. THE EFFECT OF SVEGM ON THE SEISMIC RESPONSE OF THE DAM

In the following, the response of the dam for different types of input motions introduced in Table 2 will be compared in terms of acceleration and displacement fields. The main purpose of this section is to highlight the differences in the response of the dam between uniform and SVEGM excitations.

a) Acceleration field

The variation of acceleration response of the dam with depth is compared in Fig. 9 for all loading cases introduced in Table 2. Comparisons are in terms of the Root Mean Square (RMS) of the computed acceleration time histories. Two trends are worthy of note from this figure. First, in the case of the input acceleration time histories compatible with the Types 1 and 2 response spectra, the use of identical ground motion overestimates the acceleration responses of the dam at all elevations. Specifically, the Uniform-

Type 1 and 2 excitations result respectively in 5%-15% and 10%-30% higher acceleration intensities along the centre line of the dam than those obtained for the SVEGM-Type 1 and 2 excitations. The above trend is qualitatively valid for Type 3 input motions at lower elevations of the dam but not at near the crest of the dam. Specifically, compared to the SVEGM-Type3 input motion, the Uniform-Type3 motion yields 8% lower acceleration RMS at the crest of the dam. In practice, this may be a rather negligible difference in acceleration responses. Thus, as a general trend, it can be observed that in most elevations the ground motion incoherence causes the lower acceleration responses within the core of the dam.

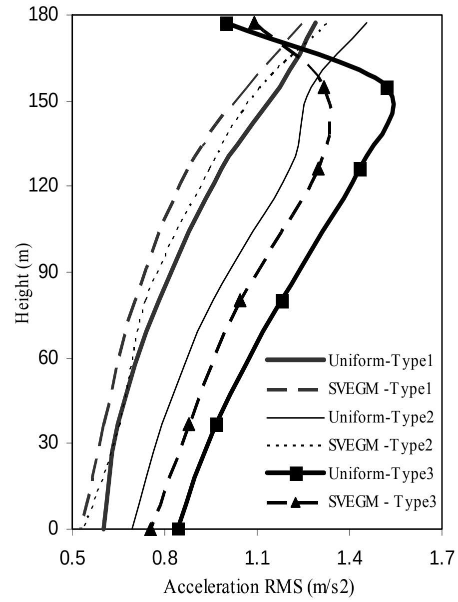

Fig. 9. The distribution of acceleration responses RMS with depth for uniform and SVEGM Excitations

From the above observation, it may be mentioned that the differences in the responses of the dam between the uniform and SVEGM excitations do depend on the characteristics of the target response spectra used in simulation process. To evaluate this tendency in a more quantitative manner, the response ratios for different loading cases were computed by dividing acceleration RMS responses due to uniform excitations by those due to SVEGM excitations and are shown in Fig. 10. It is clear that Type 2 input motions result in larger response ratios, i.e., larger differences in the acceleration responses of the dam between uniform and SVEGM excitations. It should be noted that the frequency ranges of maximum spectral values are between 2.6-6.7 Hz, 1.8-6.7 Hz and 1.1-5 Hz for Types 1, 2 and 3 input motions, respectively. It is clear that this range is wider for Type 2 input motions. Thus, the Type2-SVEGM excitations consist of more incoherent components with higher amplitudes under which the differences in the acceleration responses between uniform and SVEGM excitations increase considerably. On the contrary, the response differences between the uniform and SVEGM excitations are smaller for Types 1 and 3 motions which have maximum spectral values in a relatively smaller frequency bandwidth.

The second observation is that at lower elevations along the centre line of the dam, the Uniform-Type3 input motion produces 30%-50% and 19%-23% higher acceleration responses than those of Uniform-Type1 and Uniform-Type2 input motions, respectively. Similarly, at lower elevations, SVEGM-Type3 input excitations produce respectively 24%-50% and 20%-42% higher acceleration responses than those of SVEGM-Type1 and SVEGM-Type2 motions. This can be explained by considering the first natural frequency of the dam which falls within the frequency range of the maximum spectral values of Type 3 input motions (1.1-5 Hz) and thus more energy is delivered to the dam system. The characteristics frequency (period) of the dam model is about 1.1 Hz (0.9 s), which is in good agreement with the results of in-situ tests [20].

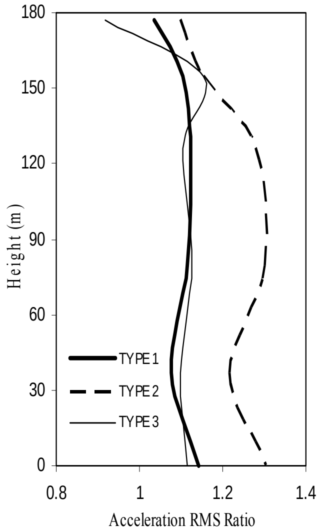

Fig. 10. The distribution of acceleration RMS ratios with depth for different types of input motions

The situation is vice versa at the upper elevations of the dam where the crest acceleration intensities due to Uniform-Type3 and SVEGM-Type3 input motions are respectively 23% and 13% smaller than those of Uniform-Type1 and SVEGM-Type1 input motions; and 31% and 18% smaller than those of Uniform-Type2 and SVEGM-Type2 input motions. This can be attributed to the marked plastic behaviour of the dam body due to Type 3 input motions under which the attenuation of waves becomes more effective and consequently the acceleration intensities decrease when passing towards the crest. To shed light on this aspect, the distribution of plastic zones in the dam body is shown in Fig. 11 for three types of uniform excitations, at the time when the peak acceleration is reached at the crest. As can be seen, due to Uniform-Type3 input motion more plastic zones are developed in the core and upstream of the dam. The similar tendency was addressed by Ebrahimian and Vafaeian [24] who studied the seismic response of earth dams under different types of earthquakes.

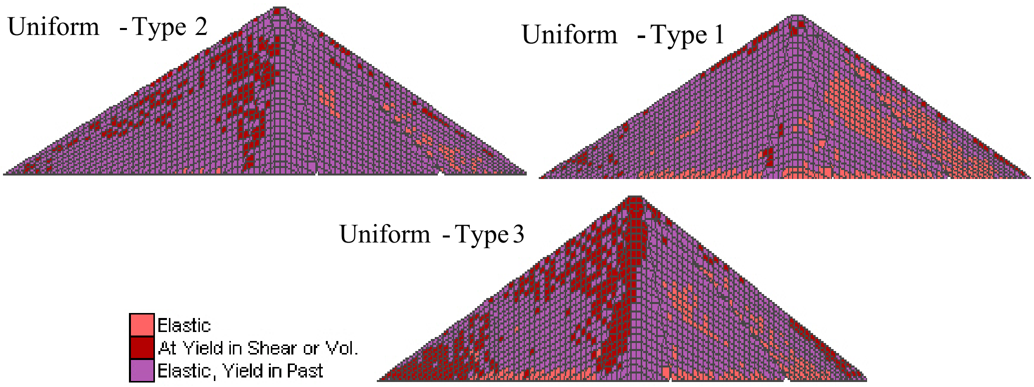

Fig. 11. Distribution of plastic zone development in the dam body at the time when peak acceleration is reached at the crest

b) Displacement field

Figure 12 shows the time histories of vertical displacements at the dam crest for different loading cases. As can be seen, the Uniform-Type3 input motion results in about 3 and 2.1 times larger settlements than those of Uniform-Type1 and Uniform-Type2 excitations. The same tendency is valid for SVEGM-Type3 input motion which results in about 2.4 and 2.1 times larger settlements than those of SVEGM -

Type1 and SVEGM -Type2 excitations, respectively. From this observation it may be mentioned that, both uniform and SVEGM input motions with lower frequency content produce the larger permanent settlements in the crest of the dam.

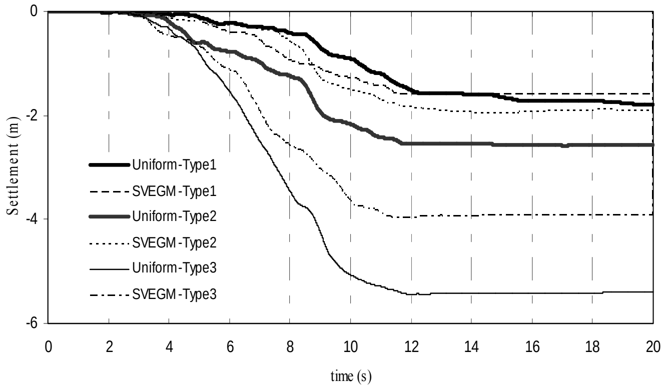

Fig. 12. Vertical displacement time history computed at the crest of the dam for three types of uniform and SVEGM excitations

Considering Fig. 12, an important trend is worthy of note. As can be seen, compared to SVEGM input motions, uniform input motions conservatively overestimate the crest settlements of the dam. Therefore, it can be inferred that the effect of ground motion incoherence reduces the vertical displacements of the crest of the dam. More specifically, the Uniform-Type 1, 2 and 3 excitations overestimate the crest settlements by as much as 10%, 35% and 40%, respectively. Thus, it can be mentioned that, for low frequency excitations (Types 2 and 3 motions), the incoherence effect is more manifested, and thus more reduction in the crest settlements for SVEGM excitations can be observed.

Figure 13 compares the maximum horizontal displacement profiles computed under uniform and SVEGM excitations. It is found from this figure that for Uniform-Type 2 and 3 excitations, the crest displacements are respectively 2 and 1.7 times larger as compared to those of SVEGM-Type 2 and 3 excitations. On the contrary, for Type 1 motions, the displacement response differences between the uniform and SVEGM excitations does not take place considerably. Therefore, similar to the trend discussed for settlement response, it can be concluded that the effect of ground motion incoherence is more conspicuous for low frequency excitations under which greater difference in the displacement responses between SVEGM and uniform excitations can be observed.

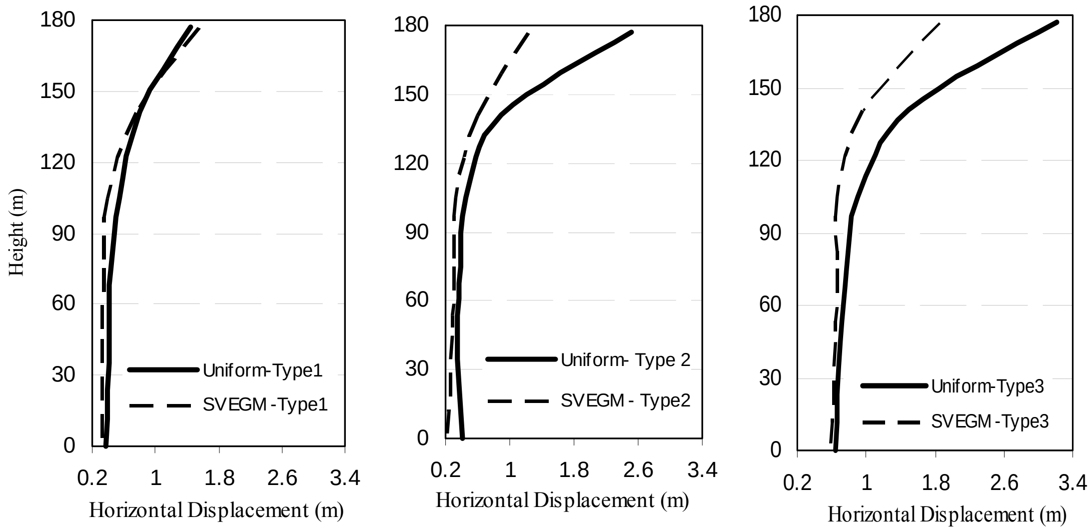

Fig. 13. Maximum horizontal displacement profile computed along the dam centre line for three types of uniform and SVEGM excitations

In this study, the permanent displacement of sliding blocks on the Masjed Soleyman dam is calculated using the Newmark's [25] method for selected potential surface. This simplified method includes two steps:

1- Perform a dynamic analysis of the dam assuming that the failure surface does not exist. Determine the time history of an average acceleration for the soil above the failure surface

2- Use this average time history of acceleration as input to a sliding block analysis and compute the resulting permanent slip along failure surface.

The adopted sliding surface for the upstream side of the dam is shown in Fig. 2. Permanent displacement analysis results for uniform and SVEGM input motions are shown in Fig. 14. As can be seen, in unison with the trend discussed above, the SVEGM excitations result in about 1.2 to 3 times smaller displacements as compared to those obtained under uniform motions. In other words, the uniform excitation conservatively results in larger permanent displacements. The displacement response trends observed in this study are in general agreement with the Chen and Harichandran [7] results in the sense that the displacements and strains obtained by uniform excitations are slightly conservative within the core and are acceptable.

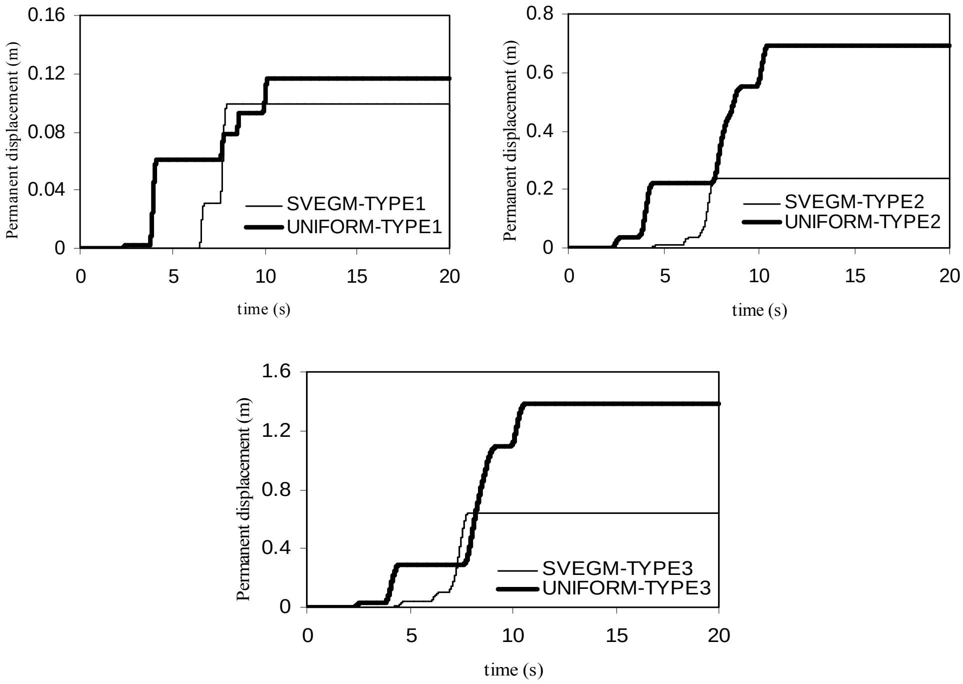

Fig. 14. Permanent displacement calculated using the sliding block analysis for different types of uniform and SVEGM excitations

6. CONCLUSION

In order to investigate the influence of frequency content of input motions on the response of the dam to multi-support excitations, the non-uniform acceleration time histories are generated based on three different target response spectra. It is observed that compared to Type 1 and 2 input motions, Type 3 input motions produce up to 50% and 42% higher acceleration responses at the lower parts of the dam, respectively. This can be explained by considering the natural frequency of the dam which falls within the frequency range of the maximum spectral values of Type 3 input motions. On the other hand, the smallest crest acceleration amplification is observed under Type 3 input motions during which the plastic behaviour of the dam body is substantial. Consequently, the acceleration intensities decrease when passing towards the crest. It is also found that the uniform input motions generated compatible with the Types 1 and 2 response spectra result in a 5%-15% and 10%- 30% higher acceleration responses than those of multi-support excitations. The above trend is qualitatively valid for Type 3 input motions at lower elevations of the dam but not at the crest of the dam where the uniform excitation yields slightly lower acceleration response. Besides, it is found that the uniform input motions compatible with the Types 1, 2 and 3 response spectra, respectively overestimate the crest settlements by as much as 10%, 35% and 40%. The same trend is observed for horizontal displacements. The results indicate that the decreased effect of ground motion incoherence on displacement responses of the dam is more conspicuous for long period components of input motions. The SVEGM excitations result in 1.2 to 3 times smaller permanent displacement of sliding mass as compared to those obtained under uniform motions. As a general trend, it can be expressed that the traditional assumption of uniform earthquake ground motion conservatively overestimates displacement and acceleration responses of the dam.

Acknowledgements: This paper is a part of the research project with the title of “Effect of spatial variation of Earthquake Ground Motion on Dynamic Behaviour of Embankment Dams” funded by the International Institute of Earthquake Engineering and Seismology (IIEES) under activity code of 6128 and project code of 450. This support is gratefully acknowledged.

REFERENCES

1. Harichandran, R. S. (1991). Estimating the spatial variation of earthquake ground motion from dense array recordings. *Struct. Safety*, Vol. 10, pp. 219–233.
2. Newmark and Rosenblueth, (1971). *Fundamentals of earthquake engineering*. Prentice Hall, Englewood Cliffs, NJ.
3. Shinozuka, M., Saxena, V. & Deodatis, G. (2000). Effect of spatial variation of ground motion on highway structures. MCEER-00-0013.
4. Davoodi, M., Jafari, M. K. & Sadrolddini, S. M. A. (2012). Effect of Multi-support excitation on seismic response of embankment dams. *Int. J. of Civil Eng*, Vol. 10, No. 2.
5. Maheri, M. R. & Ghaffarzadeh, H. (2002). Asynchronous and non-uniform support excitation analysis of large structures. *Journal of Seismology and Earthquake Eng. JSEE*, Vol. 4, No. 2, 3, pp. 63-74.
6. Haroun, M. A. & Abdel-Hafiz, E. A. (1987). Seismic response analysis of earth dams under differential ground motion. *Bul. Seism. Soc. Am*., Vol. 77, No. 5, pp. 1514-1529.
7. Chen, M. T. & Harichandran, R. S. (2001). Response of an earth dam to spatially varying earthquake ground motion. *J. Engrg. Mech*., Vol. 127, No. 9, pp. 932-939.
8. Gazetas, G. & Dakoulas, P. (1992). Seismic analysis and design of Rockfill dams:state-of-the-art. *Soil Dyn Earthq Engng*. Vol. 11, pp. 27–61.
9. Davoodi, M. & Javaheri, A. (2008). Evaluating the stability of Masjed Soleiman dam sliding surfaces in uniform and SVEGM excitations. *JSEE*, Vol. 9, No. 4, pp. 229-239 (in Persian).
10. Alves, S. W. & Hall, J. F. (2006). Generation of spatially nonuniform ground motion for nonlinear analysis of a concrete arch dam. *Earthquake Engineering & Structural. Dynamics*, Vol. 35, No. 11, 1339-1357.
11. Gazetas, G., Debchaudhury, A. & Gasparini, D. A. (1982). Stochastic estimation of the non-linear seismic response of earth dams. *Soil Dyn. Earthq. Eng*., Vol. 1, pp. 39-46.
12. Popescu, R. (2002). Finite element assessment of the effects of seismic loading rate on soil liquefaction. *Can. Geotech. J*., Vol. 39, No. 2, pp. 331–344.
13. Cacciola, P. & Deodatis, G. (2001). A method for generating fully non-stationary and spectrum-compatible ground motion vector processes. *Soil Dyn. Earthq. Eng.*, Vol. 31, No. 3, pp. 351-360.

14. Deodatis, G. (1996). Non-stationary stochastic vector processes: seismic ground motion applications. *Probab. Eng. Mech*., Vol. 11, pp. 149–168.
15. Mahab-Ghods, Final Report (1994). Seismic hazard analysis of godar-E-landar site. Mahab- Ghods Consulting Engineer, Tehran, Iran.
16. Harichandran, R. S. & Vanmarcke, E. H. (1986). Stochastic variation of earthquake ground motion in space and time. *J. Engrg. Mech*., Vol. 112, pp. 154–74.
17. Harichandran, R. S. & Wang, W. (1990). Effect of spatially varying seismic excitation on surface lifelines. *Proceedings of Fourth U.S. National Conference on Earthquake Engineering*, May 20-24, Palm Springs, Vol. 1, pp. 885-894.
18. Jennings, P. C., Housner, G. W. & Tsai, N. C. (1968). *Simulated earthquake motions*. Tec. report, Earthq. Eng. Research Laboratory, California Institute of Technology, Pasadena, CA.
19. Nippon, K. & Moshanir, L. (1999). Masjed-E-Soleiman HEEP report on dynamic analysis for the Masjed-E-Soleiman Dam.
20. Jafari, M. K. & Davoodi, M. (2006). Dynamic characteristics evaluation of Mmasjed Soleiman dam using in-situ dynamic tests. *Can. Geotech. J*., Vol. 43, No. 10, pp. 997-1014.
21. Kuhlemeyer, R. L. & Lysmer, J. (1973). Finite element method accuracy for wave propagation problems. *J. Soil Mech Found*., Vol. 99, No. 5, pp. 421–7.
22. Jansen, R. B. (1988). *Advanced dam engineering for design, construction, and rehabilitation*. ISBN: 0442243979, Pub Kluwer Academic Pub.
23. Rakhshandehroo, G. & Bagherieh, A. (2006). Three dimensional analysis of seepage in 15-KHORDAD dam after impoundment. *Iranian Journal of Science & Technology, Transaction B: Engineering*, Vol. 30, No. B1.
24. Ebrahimian, B. & Vafaeian, M. (2005). Effects of dam height on the seismic response of earth dam. *Proceeding of 7th International Conference on Civil Engineering*, Tarbiat Modarres University, Tehran, Iran.
25. Newmark, N. M. (1965). Effects of earthquakes on dams and embankments. *Geotechnique*, Vol. 15, No. 2, pp. 139–60.